Observing the dynamic variation of the binding force between rhodostomin ligand and integrin alpha (IIb) beta (3) receptor using a photonic force microscope

Bo-Jui Chang [*a], Chia-Fen Hsieh[c], Chi-Hung Lin[c], Sien Chi[a], Long Hsu[b]
[a]Institute of Electro-Optical Engineering, National Chiao-Tung University, Hsinchu, Taiwan
[b] Department of Electrophysics, National Chiao-Tung University, Hsinchu, Taiwan
[c]Institute of Microbiology and Immunology, National Yang Ming University, Taipei, Taiwan

ABSTRACT

The conformational change of integrin $\alpha_{IIb}\beta_3$ plays an important role in clot formation. However, the correlation between the structure and the function of integrin $\alpha_{IIb}\beta_3$ in interacting with its ligand is still not clear. In this report, we focus on the dynamic variation of the binding between integrin $\alpha_{IIb}\beta_3$ and its ligand, rhodostomin by using a photonic force microscopy (PFM). The PFM is used to trap a rhodostomin-coated bead and, then, shift it to bind a surrounding CHO $\alpha_{IIb}\beta_3$ cell. Meanwhile, it tracks, with a resolution of 1MHz, the Brownian fluctuations of the trapped bead. Theoretically, the smaller the amplitude of the Brownian fluctuations, the stronger the stiffness of the binding force between the rhodostomin and the CHO $\alpha_{IIb}\beta_3$ cell. Experimentally, a significant decrease of the Brownian fluctuations was observed during the interval between the 360th seconds and the 400th seconds after the trapped rhodostomin-coated bead contacted an integrin-expressed CHO $\alpha_{IIb}\beta_3$ cell. This observation reveals that it takes the rhodostomin 360 seconds to seek the correct position to bind to the integrin $\alpha_{IIb}\beta_3$. After 400 seconds, the rhodostomin has bound rigidly with the integrin $\alpha_{IIb}\beta_3$. We presume that the integrin $\alpha_{IIb}\beta_3$ has reached its final stage of conformational change.

Keywords: optical tweezers, photonic force microscope, integrin $\alpha_{IIb}\beta_3$, rhodostomin, ligand and binding force

1. INTRODUCTION

It is interesting that our blood normally flows fluidly but coagulates when we have wounds. The coagulation of blood at the wounds is due to the aggregation of platelet. And the aggregation of platelets includes a lot of signal processings and molecular interactions inside and outside the platelets, especially via integrin $\alpha_{IIb}\beta_3$. For example, wounded cells will release signals such as thrombin and ADP to platelets. As shown in Fig. 1, the thrombin and ADP will then bind to their specific receptors on the platelets. This will induce an inside-out signal to activate integrin $\alpha_{IIb}\beta_3$[1] to bind to its natural ligand, fibrinogen. Importantly, this trigger signal also induces the conformational change of the platelets. As a result, the platelets aggregate.

Because the platelets are not easy to be cultured, we clone integrin $\alpha_{IIb}\beta_3$ from platelets into the Chinese Hamster Ovary (CHO) cells for growing. Note that the cloned integrin $\alpha_{IIb}\beta_3$ is not activated without thrombin and ADP. Therefore, Fig. 2(a) shows that mixing the cloned integrin $\alpha_{IIb}\beta_3$ with fibrinogen ligand alone can not cause platelets aggregation. Fortunately, there is another kind of ligand, snake venom rhodostomin, which alone can bind to and activate the integrin $\alpha_{IIb}\beta_3$ on living cell.[2, 3] Therefore, binding rhodostomin ligand to a non-activated integrin $\alpha_{IIb}\beta_3$ on the CHO cell will result in platelets aggregation. Fig. 2(b) shows the cells aggregation caused by the rhodostomin-induced activation of integrin $\alpha_{IIb}\beta_3$, which proves the feasibility of our biological model.

The process of platelet aggregation can be roughly separated into two parts; namely, the activation of the integrin $\alpha_{IIb}\beta_3$ and the clustering of the integrin $\alpha_{IIb}\beta_3$. Although many studies have been conducted to elucidate the mechanisms of platelets aggregation, their results mostly arise from the experiments based on whole-cell interaction assays and the interaction of integrins with specific monoclonal antibodies[4-6]. Detailed interaction between a single integrin $\alpha_{IIb}\beta_3$ and

Optical Trapping and Optical Micromanipulation, edited by
Kishan Dholakia, Gabriel C. Spalding, Proceedings of SPIE Vol. 5514
(SPIE, Bellingham, WA, 2004) · 0277-786X/04/$15 doi: 10.1117/12.559501

its ligand has not been ever explained. In this report, we focus on the dynamic variation of the binding between integrin $\alpha_{IIb}\beta_3$ and rhodostomin, a snake venom protein, by using a photonic force microscope (PFM) [7].

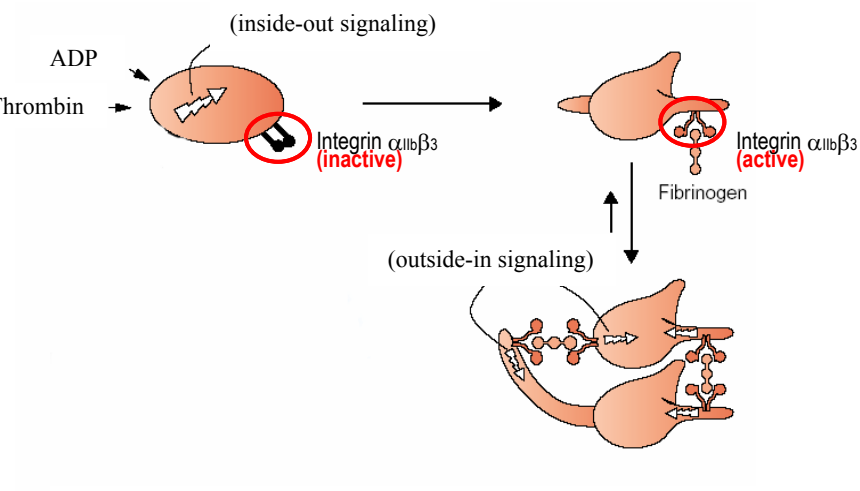

Fig. 1 The mechanism of platelets aggregation. This figure is referred to "Current opinion in cell biology", 13：546-554, 2001.

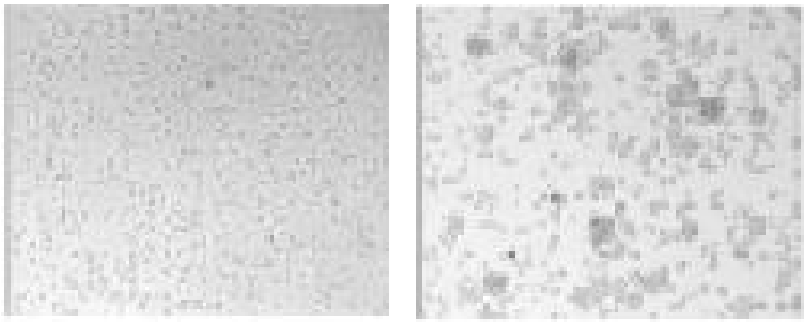

Fibrinogen Rhodostomin

Fig. 2 (a) Cells do not aggregate with fibrinogen since the integrin $\alpha_{IIb}\beta_3$ is not activated. (b) Cells aggregate with rhodostomin.

PFM, first developed by E. Stelzer of European Molecular Biology Laboratory, is an advanced version of optical tweezers[8]. Equipped with an optional high-sensitivity quadrant photo detector (QPD), PFM is capable of trapping a micro object and monitoring the prompt and random Brownian fluctuations of the trapped object simultaneously. In principle, the amplitude of the Brownian fluctuations of the trapped object reflects the stiffness of the binding force exerted upon it: the smaller the amplitude of the Brownian fluctuations, the stronger the stiffness of the binding force. Our PFM exhibits a spatial resolution of a few nanometers at an acquisition rate over 1*MHz*. Therefore, our PFM is an ideal platform for the measurement of the adhesion or binding force between molecules, cells, or bacteria.

In this experiment, we use the optical tweezers of our PFM to trap a bead whose surface is coated with rhodostomin. Then, we shift the trapped bead to contact with a CHO cell that expresses exogenous integrin $\alpha_{IIb}\beta_3$ on their plasma membranes[9]. Subsequently, we record the Brownian fluctuations of the trapped bead by tracking the forward scattering light from the bead with the QPD of our PFM. By analyzing the recorded fluctuations via a series of statistical analysis such as power spectra, histogram, and autocorrelation[10], we expect to obtain the dynamic variation of the three

components of the three-dimensional stiffness, k_x, k_y, and k_z, of the binding force between the rhodostomin and the integrin-expressed CHO $\alpha_{IIb}\beta_3$ cell. Because the binding affinity is presumably related to the conformational change of integrin, this PFM technique is ideal for the direct study for the individual binding affinity between an integrin and its ligand *in vivo* at 1*MHz* resolution. However, so far, we are not able to finish the calculation for the stiffness of the binding force yet. Nevertheless, we have observed the dynamic change of Brownian fluctuations of the rhodostomin-coated bead interacting to the CHO $\alpha_{IIb}\beta_3$ cells for 500 seconds.

2. MATERIAL

2.1 Cells and transfectants

EcR Chinese Hamster Ovary (CHO) cells were stably co-transfected with cDNA that encoded human integrin subunits α_{IIb} and β_3. EcR CHO were grown in Hams F12 medium supplemented with 10% fetal bovine serum, 2 mM L-glutamine, and 1% Pen-Strep.

2.2 Rhodostomin-coated micro-particles

Recombinant rhodostomin was produced according to the protocols described previously (Chang *et al*., 1997). Beads were coated with recombinant rhodostomin proteins by physical hydrophobic adsorption method. Essentially, polystyrene beads were incubated with 0.1mg/mL rhodostomin in phosphate buffered saline (PBS) for 3 hr at 4°C with gentle mixing, washed with PBS for three times, and further incubated with 5% bovine serum albumin (BSA) for 3 hr at 4°C.

2.3 Immunofluorescence staining

Glass coverslips were coated with 1 mg/ml collagen at 37°C for 30 min before EcR CHO cells were grown to confluence. To visualize the transfected membrane proteins, cells were fixed, permeabilized, and labeled with monoclonal antibodies made against human integrin β_3 (CHEMICON MAB1974) or integrin α_{IIb} (CHEMICON MAB1990), followed by fluorochrome-conjugated secondary antibodies. The resulting slides, as shown in Fig. 3, were observed using a Leica TCS SP2 confocal microscope (Leica Microsystems, Heidelberg, Germany).

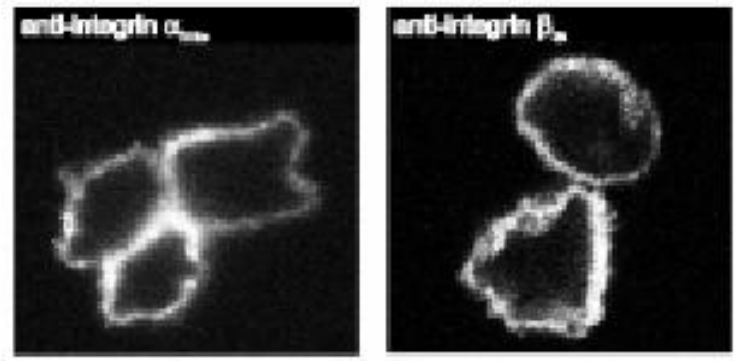

Fig. 3 Immunofluorescent analysis of the sub-cellular localization of recombinant human integrin α_{IIb} and β_3 in CHO-$\alpha_{IIb}\beta_3$ cells. The CHO-$\alpha_{IIb}\beta_3$ cells, were then fixed, permeabilized, labeled with a primary monoclonal antibody, anti-α_{IIb} and anti-β_3. The cells then were stained with Rhodamine-conjugated goat anti-mouse IgG. The experiments were imaged using a Leica TCS SP2 confocal microscope.

3. APPARATUS

3.1 Principle of Forward Scattering Detection

While the bead is being trapped by the optical tweezers of our PFM, it scatters the laser light in a random fashion. The forward scattering light generates a scattering pattern that is sensitive to the movement of the bead. By tracking the scattering pattern with the QPD of our PFM, we can distinguish the movement of the trapped bead below the limitation of Raleigh principle at nanometer resolution. Fig. 4 illustrates the principle of detecting the forward scattering pattern of the trapped bead. A laser beam is tightly focused to trap a bead by a high numerical aperture (N.A.) objective in our optical tweezers system. Part of the laser light encountering the trapped bead is randomly scattered. The forward scattering pattern is projected by an imaging lens onto the QPD of our PFM. The QPD is placed on the back focal plane of the imaging lens. Note that a QPD consists of four detectors as shown in the figure. Each detector will output an independent voltage signal, which is proportional to the intensity of the incident light upon it. As shown on the right in Fig. 4, some suitable combinations, $Signal_x$, $Signal_y$, and $Signal_z$, of the four voltage signals, V_1, V_2, V_3, and V_4, can be used to determinate the movement of the bead via this forward scattering detection.

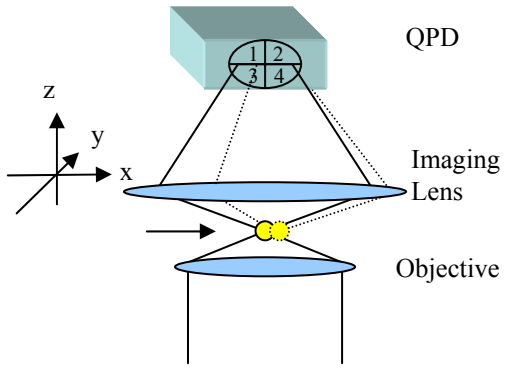

$$Signal_x = \frac{(V_1+V_3)-(V_2+V_4)}{(V_1+V_2+V_3+V_4)}$$

$$Signal_y = \frac{(V_1+V_2)-(V_3+V_4)}{(V_1+V_2+V_3+V_4)}$$

$$Signal_z = (V_1+V_2+V_3+V_4)$$

Fig. 4 The principle of forward scattering detection

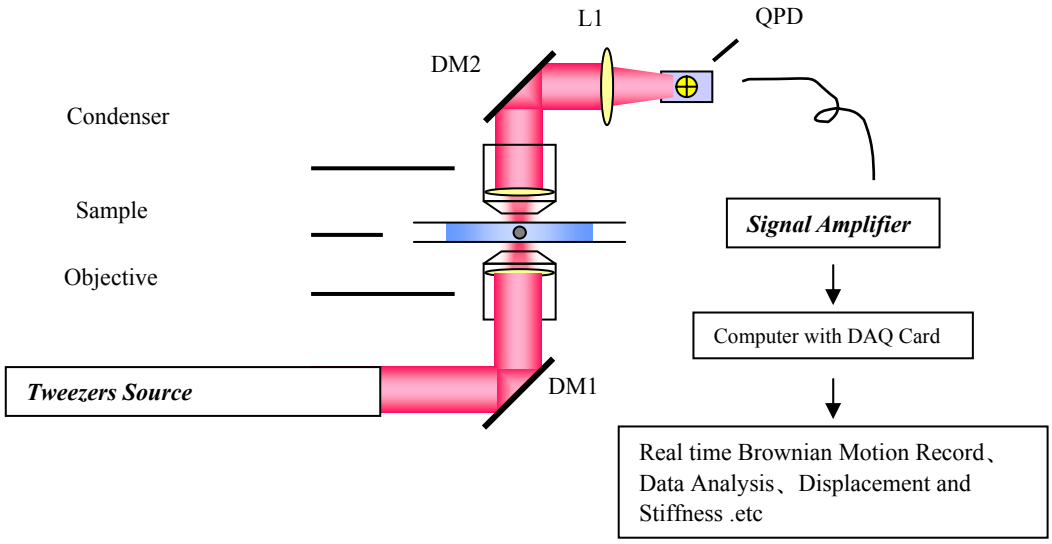

Fig. 5 The setup of our PFM system.

3.2 Setup

We construct our PFM on a Leica DMIRB microscope. The setup of our PFM is illustrated in Fig. 5. In our system, we use a diode pumped solid-state laser (CrystaLaser, 500mW, 1064nm) as the light source of the PFM. The position of the trapped bead is imaged via the forward scattering detection with a QPD (Hamamatsu multi-element photodiodes G6849), as described in section 3.1. A DAQ card (NI-6110) with a simultaneous sampling rate up to 5MHz is used to acquire the four voltage signals, V_1, V_2, V_3, and V_4, output from the QPD. DM1 and DM2 are two dichroic mirrors. L1 is an imaging lens to project the forward scattering pattern of the bead onto the QPD.

3.3 Spatial Resolution of our PFM

We calibrate the spatial resolution of our PFM by scanning a 1-μm-in-diameter bead across the focus of the laser beam. While the bead is scanning along x direction, the forward scattering pattern upon the QPD moves in x direction as well. Fig. 6 shows the signal $Signal_x$, as described in section 3.1, as a function of time. It is obvious that the peak-to-peak interval of 12 units corresponds to a distance of 1μm, which is the diameter of the bead. Because the noise level is 0.05 units, the reliability partition number is, then, approximately 240 (=12/0.05). This results in a spatial resolution of 4nm (=1μm/240) for our PFM!!

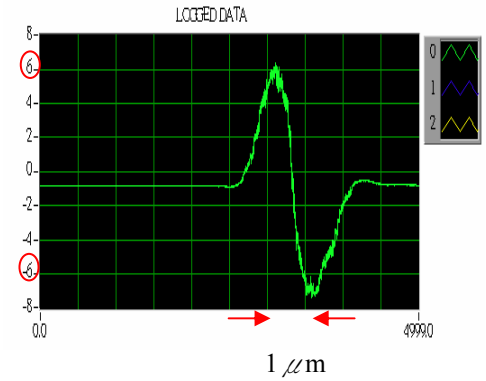

Signal level: 1$\mu m \rightarrow$ 12 units
Noise level ~ 0.05 units (Calibrated from our system.)
Reliability partition number~12/0.05=240。
Resolution ~ 1μm/240=4nm!!

Fig. 6 The signal $Signal_x$ output from the QPD as a function of time while a bead is scanned across the laser focus.

4. EXPERIMENTAL METHODS

4.1 Principles

PFM is a novel type of force microscope that uses nano- to micrometer sized beads in solution as a probe and measures the position of the bead relative to the geometric center of the laser trap with a typical spatial resolution of a few nanometers at an acquisition rate over 1MHz. In our system, by analyzing the fluctuations of the trapped bead for 5 seconds at a 200kHz-sampling rate, we are able to obtain the stiffness of the trapping force exerted upon the bead. Here, the trapping force is actually a sum of all the interaction force on the trapped bead from local environment. In principle, the larger the stiffness of the trapping force, the smaller the amplitude of the fluctuations of the trapped bead.

Unfortunately, we have not finished calibrating the force for our optical tweezers. In addition, the interacting time window between rhodostomin ligand and integrin $\alpha_{IIb}\beta_3$ receptor has not been well investigated. Therefore, we didn't really measure the binding force in this report. However, because the fluctuation of the ligand-coated bead decreases as the integrin-ligand binding affinity increases, we alternately measured the fluctuations of the rhodostomin ligand-coated bead during the activation process of the bound integrin $\alpha_{IIb}\beta_3$ expressed CHO cell. We believe that the amplitude variation of the Brownian fluctuations as a function of time reflects the dynamic variation of the corresponding binding force.

4.2 Method

To observe the dynamic variation of the binding force, we just need to observe the dynamic change of the fluctuation of the ligand-coated bead on the integrin-expressed cell. As shown in Fig. 7, we first used the optical tweezers to trap a bead and, then, shifted it to contact with an integrin-expressed cell by the side. Subsequently, we recorded the Brownian motion of the bead at a sampling rate of 10kHz for 500 seconds. Although the position of the fluctuations may change from time to time, the amplitude of fluctuations still represents the binding force. Therefore, we took the standard deviation of every 10,000 positions of the Brownian motion of the bead to represent its fluctuation amplitude per second. 5,000,000 position points were sampled and 500 fluctuation points were deduced in each 500-second experiment.

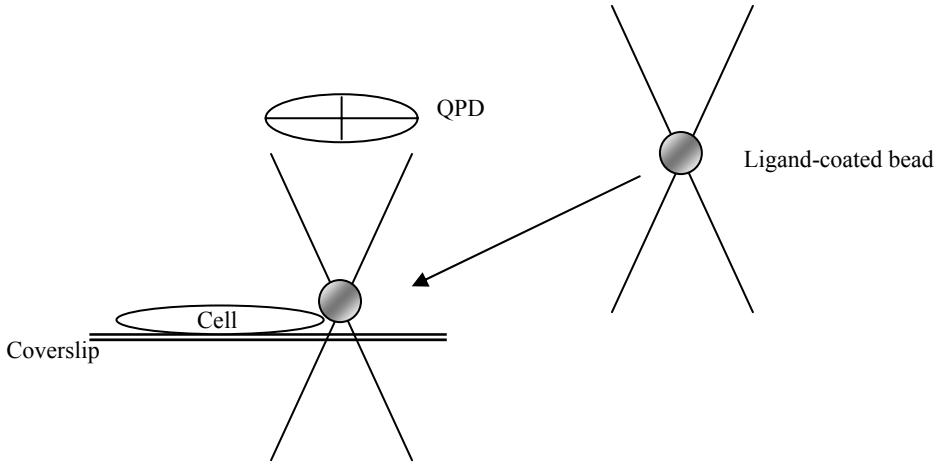

Fig. 7 The trapped Ligand-coated bead is shifted by our optical tweezers to contact with a surrounding integrin-expressed cell by the side. Once the bead touches the cell, we start recording the fluctuations of the bead.

5. RESULTS AND DISCUSSIONS

Fig. 8 shows the positions of the trapped rhodostomin-coated bead and the corresponding standard deviation of the positions within the first 500 seconds after the bead contacted with a surrounding integrin $\alpha_{IIb}\beta_3$-expressed cell. The blue, green, and red lines in Fig. 8(a) and Fig. 8(c) represent the positions of the trapped bead in *x*-, *y*-, and *z*-direction, respectively. The corresponding standard deviation of the positions are as shown in Fig. 8(b) and Fig. 8(d). Note that the standard deviation of the positions represents the amplitude of the Brownian fluctuations of the trapped bead. It can be seen that the amplitudes of the Brownian fluctuations are relatively large in the first 360 seconds, whereas the amplitudes of the Brownian fluctuations become relatively small after 400 seconds. The results in Fig. 8(b) and Fig. 8(d) are similar to each other, which represent the repeatability of our experiment.

The dynamic variation of the binding interaction is thus observed. This observation reveals that it takes the rhodostomin 360 seconds to seek the correct position to bind to the integrin $\alpha_{IIb}\beta_3$. During this interval, the binding affinity of the single rhodostomin ligand-integrin $\alpha_{IIb}\beta_3$ receptor pair slightly varies with time. This implies that the integrin $\alpha_{IIb}\beta_3$ is changing its conformation for binding. However, after 400 seconds, the rhodostomin has bound rigidly with the integrin $\alpha_{IIb}\beta_3$. And the affinity remains unchanged. We presume that the integrin $\alpha_{IIb}\beta_3$ has reached its final stage of conformational change.

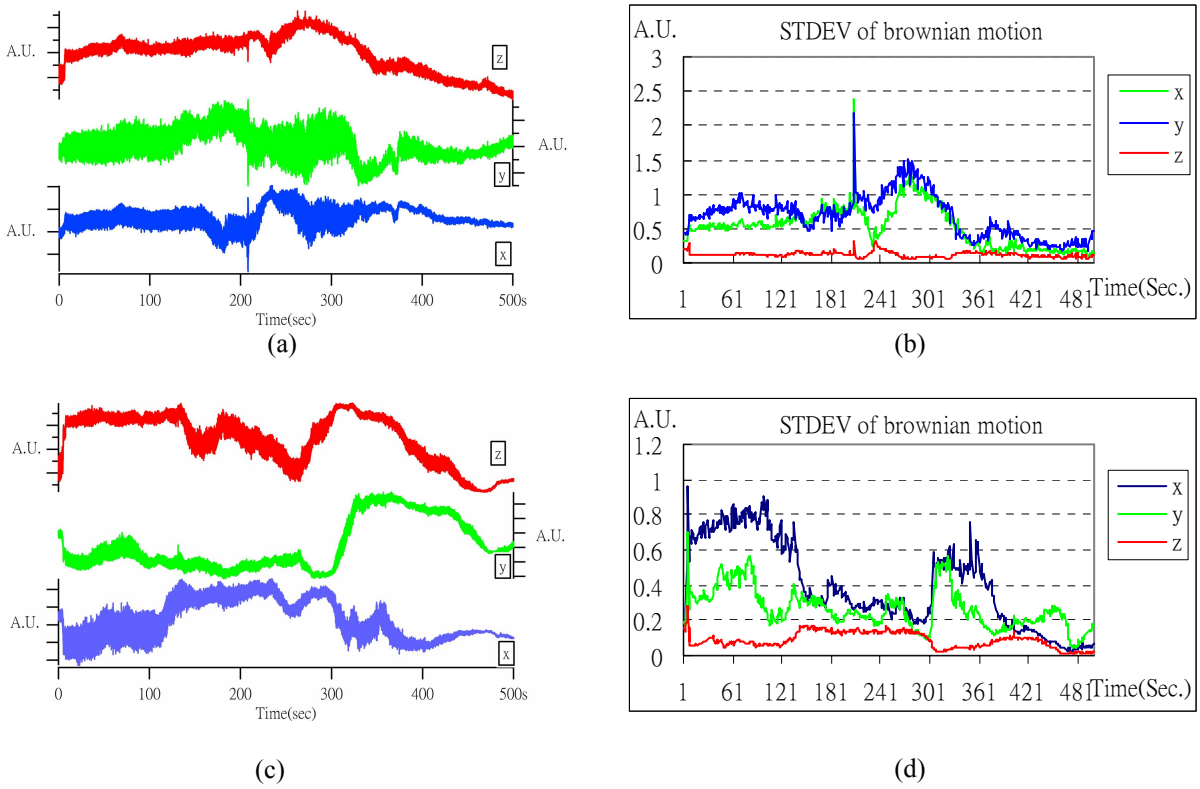

Fig. 8 The fluctuations of a rhodostomin-coated bead adhered to an $\alpha_{IIb}\beta_3$-expressed cell.
(a) and (c): the position signals of the trapped bead as a function of time.
(b) and (d): the corresponding standard deviation of the positions, which represents the amplitude of the fluctuations of the bead.

6. SUMMARY

It is an interesting and important research task to study the detailed biochemistry of receptor-ligand interactions. One typical example of this interaction is the platelet integrin $\alpha_{IIb}\beta_3$. Our goal in this experiment is to study the dynamic variation during the activation of integrin $\alpha_{IIb}\beta_3$ and its subsequent conformational change. In this report, we focus on the dynamic variation of the binding force between rhodostomin ligand and integrin $\alpha_{IIb}\beta_3$ receptor. Rhodostomin is an ideal ligand in this experiment since it can bind and activate an integrin. Therefore, we only need to clone our integrin $\alpha_{IIb}\beta_3$ on a living CHO cell.

The dynamic variation of the binding force can be observed from the fluctuations of the rhodostomin-coated bead after interacting with its integrin $\alpha_{IIb}\beta_3$. The smaller the amplitude of the fluctuations, the stronger the binding force. Although we have not finished the work to calculate for the binding force from the Brownian fluctuations data, we make use of the standard deviation of the measured fluctuations to study the dynamic variation of the binding affinity. We observe that it takes the rhodostomin 360 seconds to seek the correct position to bind to the integrin $\alpha_{IIb}\beta_3$. After 400 seconds, the rhodostomin has bound rigidly with the integrin $\alpha_{IIb}\beta_3$. We presume that the integrin $\alpha_{IIb}\beta_3$ has reached its final stage of conformational change.

REFERENCES

1. D. R. Phillips, K. S. Prasad, J. Manganello, M. Bao, L. Nannizzi-Alaimo, *Integrin tyrosine phosphorylation in platelet signaling*, Curr Opin Cell Biol **13**, 546-554, 2001.
2. H. H. Chang, W. J. Tsai, S. J. Lo, *Glutathione S-transferase-rhodostomin fusion protein inhibits platelet aggregation and induces platelet share change*, Toxicon **35**, 195-204, 1997.
3. H. H. Chang, S. J. Lo, *Full-spreading platelets induced by the recombinant rhodostomin are via binding to integrins and correlated with FAK phosphorylation*, Toxicon **36**, 1087-1099, 1998.
4. Frelinger A.L. 3rd, Cohen I, Plow E.F. , Smith M.A. , Roberts J, Lam S.C. , Ginsberg M.H., *Selective inhibition of integrin function by antibodies specific for ligand-occupied receptor conformers*, J Biol Chem **265**, 6346-6352, 1990.
5. Frelinger A.L. 3rd, Du X.P. , Plow E.F. , Ginsberg M.H. , *Monoclonal antibodies to ligand-occupied conformers of integrin alpha IIb beta 3 (glycoprotein IIb-IIIa) alter receptor affinity, specificity, and function*, J Biol Chem **266**, 17106-17111, 1991.
6. Datta A, Huber F, Boettiger D, *Phosphorylation of beta3 integrin controls ligand binding strength*, J Biol Chem **277**, 3943-3949, 2002.
7. E. –L. Florin, A. Pralle. J. K. H. Hörber and E. H. K. Stelzer, *Photonic force microscope (PFM) based on optical tweezers and two-photon excitation for biological applications*, Journal of Structural Biology **119**, 202-211, 1997.
8. A Ashkin, J. M. Dziedzic, J. E. Bjorkholm and Steven Chu, *Observation of a single-beam gradient force optical trap for dielectric particles*, Optics Letters **11**, 288-290, 1986.
9. T. E. O'Toole *et al.*, Cell Regul **1**, 883-93, 1990.
10. Koen Visscher, Steven P. Gross, and Steven M. Block, *Construction of Multiple-Beam Optical Traps with Nanometer-Resolution Position Sensing*, IEEE Journal of Selected Topics in Quantum Electronics **2**(4), 1066-1076, 1996.

*bojui.ep88g@nctu.edu.tw; phone 886 3 571-2121ext56165; fax 886 3 572-5230; Institute of Electro-Optical Engineering, National Chiao-Tung University